Molecular-dynamics determination of electronic and vibrational spectra, and equilibrium structures of small Si clusters

Otto F. Sankey and David J. Niklewski
Department of Physics, Arizona State University, Tempe, Arizona 85287-1504

D. A. Drabold and John D. Dow
Department of Physics, University of Notre Dame, Notre Dame, Indiana 46556
(Received 26 January 1990)

We have used a new, approximate method for computing total energies and forces in covalent systems and investigated the electronic and vibrational spectra and equilibrium structures of small Si clusters (Si_n with $n=2-7$). The method uses an electronic-structure tight-binding formalism based on density-functional theory within the pseudopotential scheme. Slightly excited pseudo-atomic-orbitals are used to find the tight-binding Hamiltonian matrix in real space. Unlike other simplified tight-binding schemes, no parameters or fits to data are introduced. Forces are determined from the total-energy functional, so that molecular-dynamics simulations can be performed. The molecular-dynamics simulations yield the ground-state structure, and the vibrational spectrum. Excellent overall agreement is found with experiment and other first-principles calculations for Si clusters. The technique is immediately transferable to bulk systems and surfaces.

I. INTRODUCTION

The strength and nature of the covalent bond between two atoms critically depends on the local environment around the bonding atoms. For instance, various forms of hybridization, such as sp^2 or sp^3, can be obtained depending on the local geometry. The concept of pairwise interactions, as represented by a single local two-body potential, is simply not applicable to covalent systems. This fact presents a serious obstacle toward performing realistic time-dependent simulations of complex nonequilibrium processes in covalent materials such as the formation of random networks in amorphous semiconductors, the reconstruction at a semiconductor surface, the growth of a surface, surface and bulk diffusion, and a whole range of topics in the modern design of materials and structures.

There has recently been a very large effort[1-12] to produce potentials that mimic the many-body effects of the covalent bond. These potentials are fitted to a large body of data (and can contain up to 36 adjustable parameters[11]), in the hope that they are useful for predicting new situations. Typically, however, the potentials fit one set of data (such as bulk bonding properties), but fail to reproduce another set of data (such as surface properties or cluster properties).

The effects of the environment on the covalent bonding forces are clearly rooted in the electronic structure of the bond and can be obtained directly from electronic-structure calculations. However, rigorous electronic-structure methods are extremely computer intensive and difficult to implement. There have been recent attempts to simplify the electronic structure by introducing parametrized one-electron Hamiltonian hopping matrix elements, and a suitably chosen parametrization of a two-body (or more) repulsive interaction to obtain the total energy. Chadi[13] has used such a technique quite successfully to study the structure of semiconductor surfaces. Tománek and Schlüter[14] have similarly parametrized a tight-binding Hamiltonian for the study of Si clusters. Pettifor *et al.*,[15] Paxton *et al.*,[16] and Majewski and Vogl[17] are other authors who have developed tight-binding models of the total energy to study a variety of condensed-matter properties. More recently, Chelikowsky and Redwing[18] have developed a Hamiltonian for clusters and solids. From first principles these authors calculate the one-electron eigenvalues but fitted the total energy. Tight-binding Hamiltonians have also been used in molecular-dynamics simulations. Sankey *et al.*[19] have optimized the geometry of the semiconductor (110) surface, while Allen *et al.*[20] have investigated adatom interactions at surfaces. Wang *et al.*[21] have investigated anharmonic phonons in Si through molecular dynamics using an empirical tight-binding Hamiltonian, and Khan and Broughton[22] have used the Tománek-Schlüter tight-binding Hamiltonian for Si clusters and the (100) Si surface.

We have recently developed an *approximate* first-principles electronic-structure method that very closely matches a more rigorous calculation, but greatly reduces the computational effort required.[23] The method is tight binding like, and unlike the empirical tight-binding methods just described, this new method has no adjustable parameters and is not fitted to any experimental data. The method is entirely first principles, yet is simple enough to be used for a wide variety of purposes including bulk systems, surfaces, and amorphous materials and clusters. No periodicity is required (nor are Fourier transforms of the density, etc.) because it is entirely executed in real space. Our technique has certain elements

similar to that recently proposed by Foulkes *et al.*[24]

In this paper, we use this method to determine the equilibrium structures and vibrational spectra of small Si clusters (Si_n with $n=2-7$). The technique of molecular dynamics is employed, in which the many-body classical equations of motion, $\mathbf{F}=m\,d^2\mathbf{r}/dt^2$, is solved in time, and the subsequent motion of the atoms is determined from some set of initial conditions. Equilibrium structures were found by simulated annealing and dynamical quenching (in which the system is periodically quenched by removing kinetic energy from its atoms). In finding the vibrational spectra, the velocity autocorrelation functions are Fourier transformed. The theory and techniques described in this paper are immediately transferable to condensed-matter systems, which will be dealt with in future publications.

II. ELECTRONIC-STRUCTURE THEORY

In this section, we briefly describe the theory used to determine the electronic structure and to obtain the total energy of these systems and forces between atoms. We will describe four major approximations that simplify the electronic structure tremendously, so that medium scale (~ 100 atoms or more) molecular-dynamics simulations can easily be performed. Only a brief description of the theory will be given, as a more complete description can be found in Ref. 23.

The theoretical foundation used is density-function theory. Within this rigorous ground-state theory, we make our *first* major approximations. The approximations are the use of the Hohenberg-Kohn-Sham local-density approximation (LDA) and the pseudopotential approximation. The LDA replaces the exchange-correlation energy functional by a local function of the density. We use the local exchange-correlation functional of Ceperley and Alder as parametrized by Perdew and Zunger.[25] The pseudopotential approximation replaces the core electrons by an effective potential that acts on the valence electrons. Accurate nonlocal (angular-momentum-dependent) pseudopotentials of the norm-conserving Hamann-Schlüter-Chiang type are used.[26]

In the LDA and nonlocal pseudopotential approximation, the total-energy functional is given by

$$E_{\rm tot}=T_K+\int\left[\sum_\alpha\left[V_{\rm ion}(\mathbf{r}-\mathbf{r}_\alpha)+V_{\rm nl}(\mathbf{r}-\mathbf{r}_\alpha)\right]+\frac{e^2}{2}\int\frac{n(\mathbf{r}')}{|\mathbf{r}-\mathbf{r}'|}d^3r'+\varepsilon_{\rm xc}(n)\right]n(\mathbf{r})\,d^3r\ , \tag{1}$$

where the individual terms are, respectively, the kinetic energy, the ionic local pseudopotential of the ion at r_α, the nonlocal pseudopotential, the electron-electron Hartree repulsion, and the exchange-correlation energy, which is a functional of the electron density n.

The electronic energy eigenstates ψ_i are the expanded in a tight-binding-like linear combination of pseudo-atomic-orbitals (PAO's):

$$|\psi_i(r)\rangle=\sum_{\mu,\alpha}a_i(\mu,\alpha)|\phi_\mu^{\rm PAO}(\mathbf{r}-\mathbf{r}_\alpha)\rangle\ . \tag{2}$$

The PAO's are self-consistently determined eigenfunctions of the valence electrons of the free atom in the nonlocal pseudopotential approximation and are nodeless. The pseudoatom contains only the valence electrons, so that the orbital types μ for Si are s, p_x, p_y, and p_z.

Our *second* major approximation is motivated by the need to reduce the range of interaction between atomic orbitals, and hence, greatly reduce the number of neighbors each atom (or pair of atoms) interacts with. This reduction leads to a corresponding reduction in computer time required for the calculations. We do this by slightly exciting the PAO's by imposing the boundary condition that they vanish at and outside a predetermined radius r_c. (As $r_c\to\infty$, the atom approaches the ground state.) The value of r_c that we use here and in previous work is $5.0a_B$. The motivation for this value is that it rigorously yields a third-neighbor model for matrix elements of the single-particle Hamiltonian in crystalline Si. We have found that our results are not critically dependent on the precise value of r_c as long as r_c is not too small. The kinetic energy associated with the confinement of the electron in the atom begins a sharp increase at values of r_c slightly less than $5a_B$. A plot of the Si s-orbital wave function in the pseudopotential approximation for various values of r_c is shown in Fig. 1. The curve for $r_c=8a_B$ is virtually identical to the ground-state wave function. Notice that for $r_c=5a_B$, the wave function in the bonding region is well represented, but the long-ranged tail is eliminated. In the multicenter integrals needed in this work, we do not fit the wave function to any analytic

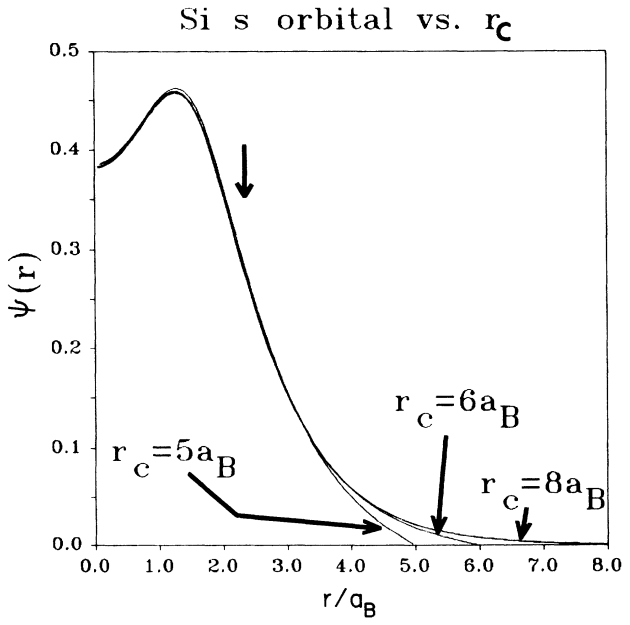

FIG. 1. The s pseudo-atomic-orbital of Si using various values of r_c. The wave function for $r_c=8a_B$ is very close to the pseudoatom ground state. The bonding region (defined to be half the nearest-neighbor distance in bulk Si) is shown by the vertical arrow.

function, but rather perform the integrals numerically from a wave-function tabulation.

The total energy in Eq. (1) can be conveniently rewritten as a sum over eigenvalues of the single-particle Hamiltonian,

$$E_{\rm tot}(n)=E_{\rm BS}(n)+[U_{ii}-U_{ee}(n,n)]+\delta U_{\rm xc}(n)\ , \quad (3a)$$

where $E_{\rm BS}(n)$ is the "band-structure" energy and is given by a sum of one-electron eigenvalues over occupied states i,

$$E_{\rm BS}(n)=2\sum_i \varepsilon_i\ . \quad (3b)$$

The quantities ε_i are the single-particle Hamiltonian eigenvalues that satisfy the Schrödinger equation in matrix form

$$\sum_{\nu,\alpha'} h_{\mu,\nu}^{\alpha,\alpha'} a_i(\nu,\alpha')=\varepsilon_i \sum_{\nu,\alpha'} S_{\mu,\nu}^{\alpha,\alpha'} a_i(\nu,\alpha')\ , \quad (4a)$$

where the single-particle Hamiltonian matrix elements are

$$h_{\mu,\nu}^{\alpha,\alpha'}=\langle \phi_\mu^{\rm PAO}(\mathbf{r}-\mathbf{r}_\alpha)|h(n)|\phi_\nu^{\rm PAO}(\mathbf{r}-\mathbf{r}_{\alpha'})\rangle\ , \quad (4b)$$

and the overlap matrix is

$$S_{\mu,\nu}^{\alpha,\alpha'}=\langle \phi_\mu^{\rm PAO}(\mathbf{r}-\mathbf{r}_\alpha)|\phi_\nu^{\rm PAO}(\mathbf{r}-\mathbf{r}_{\alpha'})\rangle\ . \quad (4c)$$

The standard single-particle LDA Hamiltonian operator is

$$h(n)=\frac{p^2}{2m}+\sum_\alpha [V_{\rm ion}(\mathbf{r}-\mathbf{r}_\alpha)+V_{\rm nl}(\mathbf{r}-\mathbf{r}_\alpha)] +e^2\int \frac{n(\mathbf{r}')}{|\mathbf{r}-\mathbf{r}'|}d^3r'+\mu_{\rm xc}(n)\ , \quad (5)$$

where $\mu_{\rm xc}(n)=d[n\varepsilon_{\rm xc}(n)]/dn$ is the exchange-correlation potential. The other terms in Eq. (3a) are the "short-ranged" repulsive potential

$$U_{\rm SR}=U_{ii}-U_{ee}(n,n) =\frac{e^2}{2}\left[\sum_{\alpha,\alpha'}{}' \frac{Z_\alpha Z_{\alpha'}}{|\mathbf{r}_\alpha-\mathbf{r}_{\alpha'}|}-\int\int d^3r\, n(\mathbf{r})\frac{n(\mathbf{r}')}{|\mathbf{r}-\mathbf{r}'|}d^3r'\right] \quad (6)$$

and an exchange-correlation correction, $\delta U_{\rm xc}$,

$$\delta U_{\rm xc}=\int n(\mathbf{r})[\varepsilon_{\rm xc}(n)-\mu_{\rm xc}(n)]d^3r\ . \quad (7)$$

The Schrödinger-like Eq. (4a) follows from a variational principle for the total energy of Eq. (1). The single-particle Hamiltonian, Eq. (5), defines a problem requiring a self-consistent solution. To avoid the difficulties associated with iterating to self-consistency, we adopt an approximation suggested by Harris.[27] Thus our *third* major approximation is to consider a sum of neutral-atom spherical charge densities as a zero-order approximation to the self-consistent density of the cluster, and to keep only first-order changes from this density in the energy functional. Thus we write

$$n(\mathbf{r})=n^0(\mathbf{r})+\delta n(\mathbf{r})\ , \quad (8)$$

where

$$n^0(\mathbf{r})=\sum_\alpha n_{\rm atom}(\mathbf{r}-\mathbf{r}_\alpha)\ . \quad (9)$$

The neutral-atom density for Si is taken to be a spherically symmetric s^2p^2 configuration. To first order in δn, the energy functional of Eq. (3a) simplifies to

$$E_{\rm tot}^{(1)}=E_{\rm BS}^{(1)}+[U_{ii}-U_{ee}(n^0,n^0)]+\delta U_{\rm xc}(n^0)\ , \quad (10)$$

where $E_{\rm BS}^{(1)}$ is the "band-structure" energy determined from the single-particle Hamiltonian of Eq. (5) with n replaced by n^0, viz., $h(n^0)$. This functional neglects terms of order δn^2.

Our approach is to use this approximate total-energy functional rather than the fully self-consistent total-energy functional. The advantages of this method are (1) the electronic eigenvalue equation only needs to be solved once for each atomic configuration instead of ~ 10 times as in a fully self-consistent calculation and (2) four-center Coulomb integrals do not need to be evaluated since they appear only in the δn^2 terms, which are neglected. This non-self-consistent method has been tested by Harris,[27] Polatoglou *et al.*,[28] and Read *et al.*[29] on metals, semiconductors, and an ionic compound (NaCl) and it is found to give surprisingly good agreement with self-consistent calculations.

Our *fourth* major approximation involves the evaluation of the matrix elements of the various terms that make up $h(n^0)$. The kinetic energy, overlap, and nonlocal part of the pseudopotential are easily evaluated exactly (numerically) for each geometry. A table of results on a fine grid of separations is constructed so that the matrix elements for any separation between the atoms is accurately interpolated. The three center matrix elements of the neutral-atom potential given by

$$V_{\rm NA}(\mathbf{r}-\mathbf{r}_\alpha)=V_{\rm ion}(\mathbf{r}-\mathbf{r}_\alpha)+e^2\int \frac{n(\mathbf{r}'-\mathbf{r}_\alpha)}{|\mathbf{r}-\mathbf{r}'|}d^3r' \quad (11)$$

are accurately approximated by an r-dependent expansion in multipole moments. The nonlinear exchange-correlation matrix elements are calculated within the average density approximation described in Ref. 23. All matrix elements are calculated in real space.

The forces are determined by differentiating the total energy $E_{\rm tot}^{(1)}$ given by Eq. (10), $\mathbf{F}_\gamma=-\partial E_{\rm tot}^{(1)}/\partial\mathbf{r}_\gamma$. The most difficult term comes from the band structure. Its derivative is

$$\frac{-\partial E_{\rm BS}^{(1)}}{\partial\mathbf{r}_\gamma}=-2\sum_{i\ ({\rm occ})}\frac{\partial}{\partial\mathbf{r}_\gamma}\langle\psi_i|h(n^0)|\psi_i\rangle =-\frac{\partial}{\partial\mathbf{r}_\gamma}\sum_{\substack{\mu,\nu\\ \alpha,\alpha'}}\rho_{\mu\nu}^{\alpha\alpha'}(h^0)_{\mu\nu}^{\alpha\alpha'} =-\sum_{\substack{\mu,\nu\\ \alpha,\alpha'}}\left[\rho_{\mu\nu}^{\alpha\alpha'}\frac{\partial(h^0)_{\mu\nu}^{\alpha\alpha'}}{\partial\mathbf{r}_\gamma}-E_{\mu\nu}^{\alpha\alpha'}\frac{\partial S_{\mu\nu}^{\alpha\alpha'}}{\partial\mathbf{r}_\gamma}\right]\ , \quad (12)$$

where $\rho_{\mu\nu}^{\alpha\alpha'}$ and $E_{\mu\nu}^{\alpha\alpha'}$ are the density and energy-density matrices, respectively,

$$\rho_{\mu\nu}^{\alpha\alpha'} = \sum_{\substack{i \\ (\mathrm{occ})}} a_i^*(\mu,\alpha) a_i(\nu,\alpha') ,$$

$$E_{\mu\nu}^{\alpha\alpha'} = \sum_{\substack{i \\ (\mathrm{occ})}} \varepsilon_i a_i^*(\mu,\alpha) a_i(\nu,\alpha') ,$$

where $a_i(\mu,\alpha)$ are the expansion coefficients of the wave function in Eq. (2).

After the forces are evaluated, the equations of motion can be solved and the positions and velocities of the atoms updated. The energy functional has been tested in bulk Si and found to give bulk static properties that are in good agreement with experiment.[23] It is the purpose of this paper to extend these calculations to the static and dynamic properties of small Si clusters using an *ab initio* molecular-dynamics technique.

III. MOLECULAR DYNAMICS

The equilibrium structures and vibrational spectra of Si clusters have been determined using the technique of molecular dynamics. The forces are calculated quantum mechanically from the total energy [Eq. (10)] and its derivatives [e.g., Eq. (12)]. The nuclear coordinates are moved in time according to the classical equations of motion, $\mathbf{F}_n = m_n \, d^2\mathbf{r}/dt^2$. These equations are integrated using the Gear predictor-corrector algorithm,[30] with a time step of ~ 1.5 fs.

The ground-state equilibrium structures are found by one of two techniques: dynamical quenching or simulated annealing. In either of these two techniques, the cluster is started in some trial structure, generally with very little symmetry.

In the technique of dynamical quenching, the atoms in the cluster are allowed to respond to internal forces and are accelerated. A kinetic temperature T_K is defined as the average classical kinetic energy of the atoms, $3/2kT_K = (1/N)\sum_i \frac{1}{2} m_i v_i^2$, where $i = 1,2,\ldots,n$ is the atom index. As the atoms accelerate, the kinetic temperature increases until a maximum is reached. The system is then quenched by setting all the velocities to zero, thus removing all the kinetic energy. The atoms again are allowed to accelerate and the quenching process is repeated. After several dynamical quenching cycles, a minimum energy configuration is obtained. The minimum may be only a local minimum, so that the procedure needs to be repeated several times with different initial configurations.

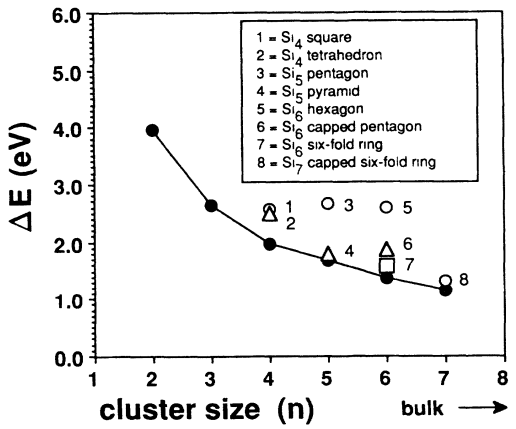

FIG. 2. The energy difference per atom between Si clusters of size $n = 2$–7 and bulk Si. The solid dots correspond to equilibrium structures explained in the text, and other metastable configurations are also shown for $n = 4$–7.

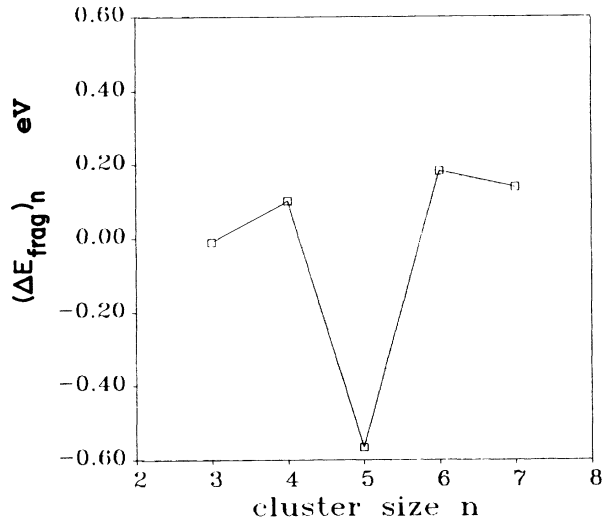

FIG. 3. The n-dependent fragmentation energy $(\Delta E_{\mathrm{frag}})_n$ as a function of n. The dip at $n = 5$ indicates that fragmentation is more likely to occur for this cluster.

In the simulated annealing technique, the energy is removed more gradually so that a global minimum is more likely to be obtained. The technique has been described by Kirkpatrick *et al.*[31] and uses the Monte Carlo algorithm of Metropolis *et al.*[32] Monte Carlo steps are taken where the coordinates of each particle are changed as $\mathbf{r}_i \rightarrow \mathbf{r}_i + \delta\mathbf{r}_i$. Here $\delta\mathbf{r}_i = r_0 \, \delta\mathbf{R}$, where $\delta\mathbf{R}$ is a triplet of random numbers between -1 and $+1$ for each atom i, and r_0 is the maximum step size. An energy difference $\delta E = -\mathbf{F}_i \cdot \delta\mathbf{r}_i$ is computed and the step is taken if $\delta E < 0$, while if $\delta E > 0$ the step is taken with probability $e^{-\delta E/kT_A}$, where T_A is an annealing temperature. This ensures that after many moves, the ensemble tends to the Boltzmann distribution. The temperature T_A is gradually reduced so that the system settles into the ground state. We have found that the dynamical quenching finds the ground state much more readily than simulated annealing for these small clusters. However, simulated annealing is more likely to find the true ground state than dynamical quenching. In either case, however, a variety of initial configurations must be tried before one can believe that the true ground state has been found.

The vibrational spectrum is found directly from the molecular-dynamics simulation without annealing or quenching. We start in a ground-state configuration and have constrained the motion so that the center of mass of the system of atoms is stationary and there is no angular momentum about the center of mass. To accomplish this, we first give the atoms random velocities commensu-

rate with a given initial kinetic temperature. In general, however, the angular momentum ($\mathbf{L}$) is nonzero. To keep the system from rotating, we adjust the velocities by subtracting the quantity $\mathbf{v}_i = (\underline{\mathbf{I}}^{-1} \cdot \mathbf{L}) \times \mathbf{r}_i$ from the velocity vector $\mathbf{v}_i$ ($i = 1, 2, \ldots, n$), where $\underline{\mathbf{I}}$ is the inertia tensor. This procedure removes the angular momentum while still allowing for randomness in the velocities. Finally the velocities are uniformly shifted so that there is no center-of-mass motion.

The frequency spectrum is determined by Fourier transforming the velocity autocorrelation function,

$$g(t) = \sum_{n=1}^{N} \frac{\langle \mathbf{v}_n(t) \cdot \mathbf{v}_n(0) \rangle}{\langle \mathbf{v}_n(0) \cdot \mathbf{v}_n(0) \rangle} .$$

Here n is the atom index and the brackets $\langle \cdots \rangle$ indi-

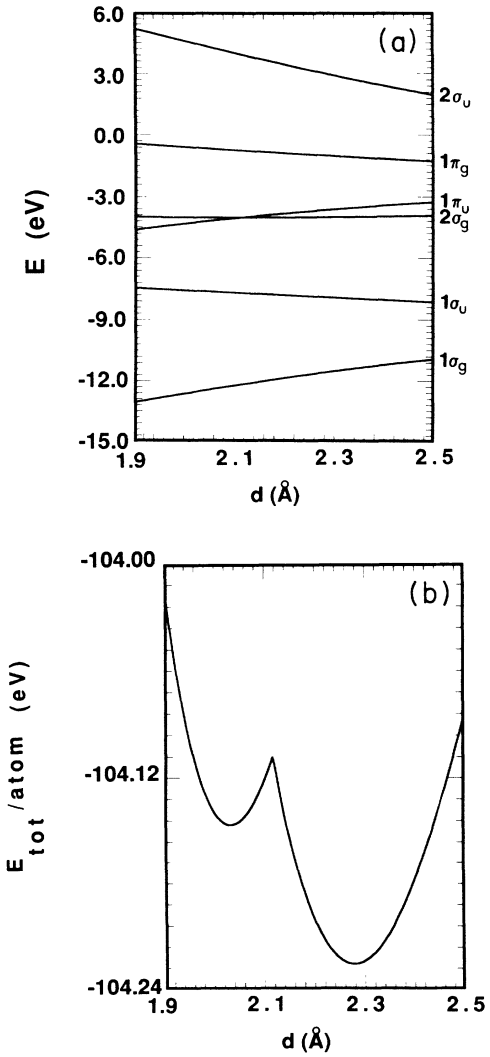

FIG. 4. (a) The one-electron LDA energy eigenvalues vs separation distance d for Si_2. The doubly degenerate (neglecting spin) $1\pi_u$ level crosses the singly degenerate $2\sigma_g$ level at about $d = 2.12$ Å. (b) Total energy per atom vs separation distance d for Si_2. A secondary minimum occurs because of the level crossing shown in (a).

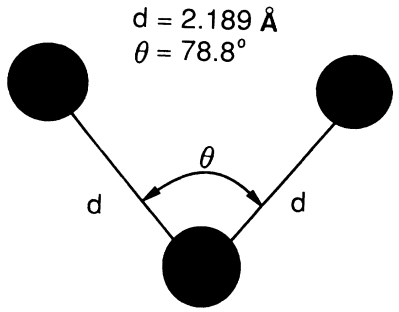

FIG. 5. The ground-state configuration of Si_3.

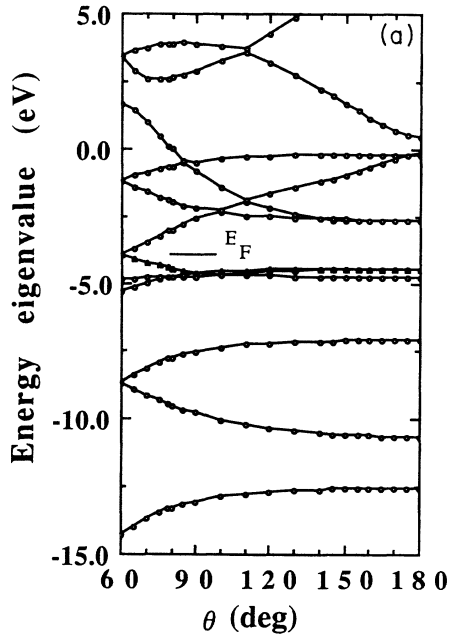

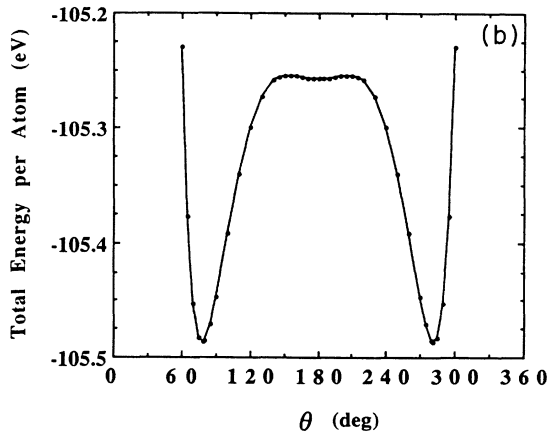

FIG. 6. (a) The one-electron LDA energy eigenvalues versus opening angle θ for Si_3, where the bond lengths d are kept constant at their equilibrium value (2.189 Å). Note the level degeneracies which occur at $\theta = 60°$, which is the highly symmetric case of an equilateral triangle. The Fermi level separating the occupied from the unoccupied levels is schematically shown. (b) Total energy per atom vs opening angle θ for Si_3 illustrating the bond bending forces of the Si_3 molecule.

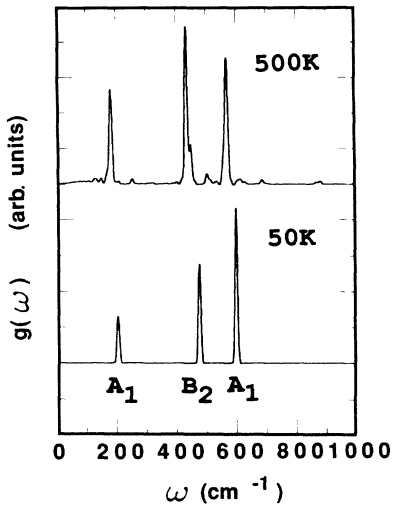

FIG. 7. Spectral density $g(\omega)$ of Si_3 in its equilibrium configuration at a low (lower figure) and a high (upper figure) kinetic temperature. The kinetic temperatures are 50 and 500 K, respectively. The modes soften at higher excitation levels, and there is added structure due to anharmonicity.

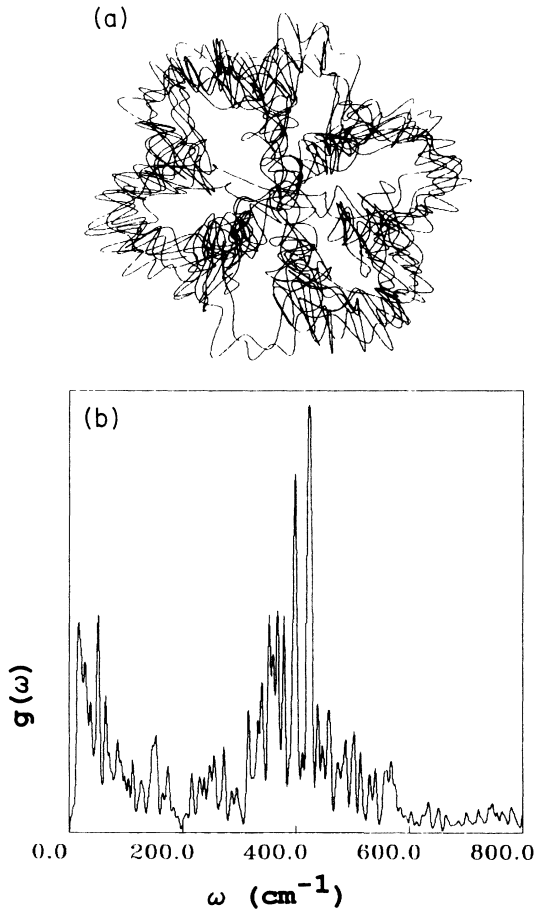

FIG. 8. (a) A snapshot of the planar motion of an Si_3 molecule at high excitation corresponding to a kinetic temperature of $\sim$2500 K. The chaotic motion is very much anharmonic. (b) The spectral density function $g(\omega)$ for the motion in (a). The three peak structure is lost and the spectrum becomes continuous.

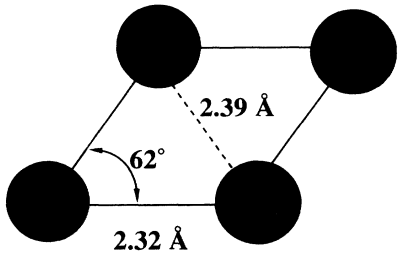

FIG. 9. The ground-state configuration of Si_4.

cate that an ensemble average over all atoms is taken. This ensemble average is defined by

$$\langle f(t_i)f(0)\rangle = \frac{1}{M-i+1}\sum_{m=0}^{M-1} f(t_{i+m})f(t_m)\ ,$$

where t_j is the time at the jth step and $j=0,1,2,\ldots,M$, with M being the total number of time steps in the simu-

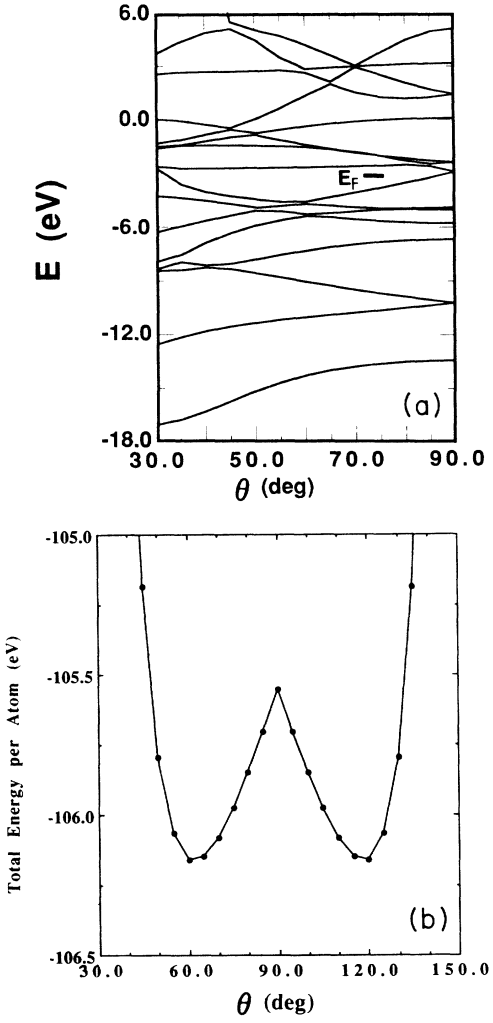

FIG. 10. (a) The one-electron LDA energy eigenvalues vs interior angle θ for Si_4. In the ground state, $\theta=62°$. The side length was kept constant at its ground-state value. Degeneracies and Jahn-Teller instabilities occur at 90°. (b) Total energy per atom vs interior angle θ for Si_4.

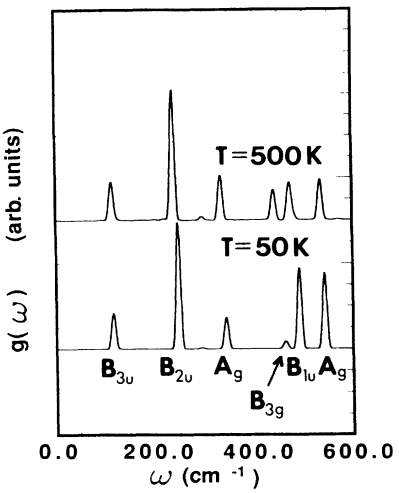

FIG. 11. Spectral density $g(\omega)$ of Si_4 in its equilibrium configuration for high and low kinetic temperatures. The peaks in the spectrum are labeled according to the symmetry of the displacements.

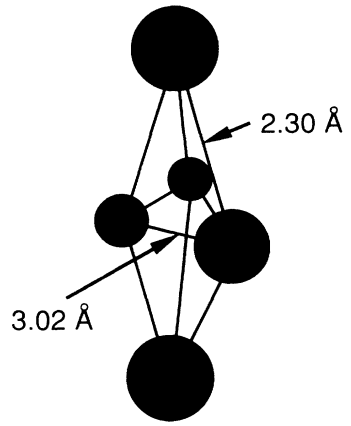

FIG. 12. Ground-state configuration of Si_5. This structure is a trigonal bipyramid, consisting of an equilateral triangle with one atom above the plane of the triangle and one atom below.

lation. The spectral density $g(\omega)$ is the Fourier cosine transform of the velocity autocorrelation function $g(t)$,

$$g(\omega)=(1/T)\int_0^T g(t)W(t)\cos(\omega t)\,dt\ ,$$

where T is the total time of the simulation. $W(t)$ is the Blackman window function[33] used to reduce oscillations due to finite time sampling.

IV. RESULTS FOR Si CLUSTERS

In this section we individually discuss the results of clusters from Si_n with $n=2$–7. We begin by summarizing the energetics of the various geometries found by quenching and annealing. In Fig. 2 we show the energy difference per atom, $\Delta E_n=(E_{\rm tot}/{\rm atom})_{\rm cluster}-(E_{\rm tot}/{\rm atom})_{\rm bulk}$, between bulk (diamond) Si and the Si clusters in their ground state and metastable equilibrium configurations.

The solid circles indicate the ground-state configurations (to be described individually), while the open circles, squares, and triangles represent local-minimum (metastable) structures. The energy per atom of the cluster approaches the bulk binding energy monotonically, but there is a marked decrease in slope in going from $n=4$ to $n=5$. This can be seen more clearly by considering the fragmentation energy as defined by Ragavachari and Logovinsky[34] according to the reaction $Si_n\rightarrow Si_{n-1}+Si$. The energy of this reaction is

$$(E_{\rm frag})_n=(\Delta E_{\rm frag})_n+[E_1-(E_{\rm tot}/{\rm atom})_{\rm bulk}]\ , \qquad (13)$$

where $(\Delta E_{\rm frag})_n=(n-1)\Delta E_{n-1}+n\Delta E_n$. The last term in Eq. (13) is a constant (independent of n). This term involves the energy of an isolated atom, which is not well described in our method because of spin effects and the use of compact orbitals.[35] The trends with n of $(E_{\rm frag})_n$ are entirely contained in the first term $(\Delta E_{\rm frag})_n$ that is plotted in Fig. 3. The lesser stability of Si_5 compared to neighboring clusters is clearly evident. The results are in very close agreement with the fragmentation trends found by Raghavachari.[36]

TABLE I. Comparison of the harmonic frequencies (in cm^{-1}) of the Si_4 molecule in this work with quantum-chemistry SCF results.

Mode symmetry	This work	6-31 G* (Ref. 43)	6-31 G
B_{3u}	116	130	137
B_{2u}	248	223	157
A_g	346	380	328
B_{3g}	464	453	371
B_{1u}	495	543	472
A_g	546	503	425

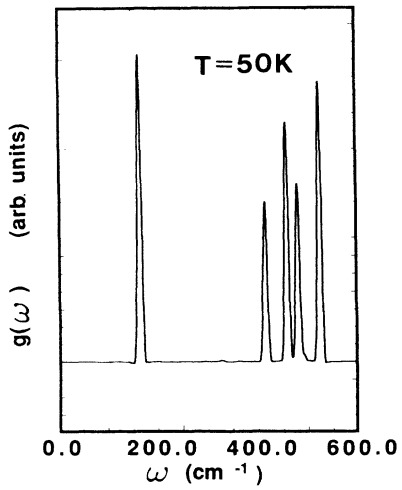

FIG. 13. Spectral density $g(\omega)$ of Si_5 in its equilibrium configuration at low kinetic temperature ($T=50$ K).

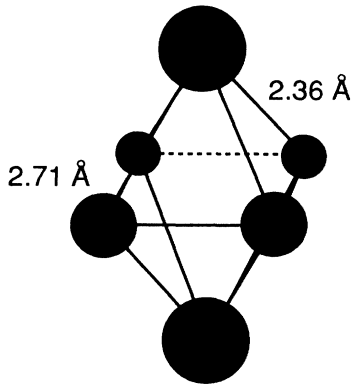

FIG. 14. Ground-state configuration of Si_6. This structure is a square bipyramid, consisting of a square with one atom above the plane of the square and one atom below.

A. Si_2

Dynamic quenching of Si_2 gives the equilibrium bond distance at $d=2.27$ Å, in good agreement with the experimental value of 2.24 Å.[37] The bulk bond length of crystalline Si is 2.35 Å, while the present theory gives 2.38 Å. Thus we find especially good agreement between theory and experiment for the large reduction in nearest-neighbor distance in going from bulk Si to Si_2 (0.11 Å experiment and 0.11 Å theory).

The single harmonic-vibrational stretch mode is determined to be $\omega=531$ cm^{-1}, which compares well to the experimental result of 511 cm^{-1}.[37] In this case at least, our results are comparable to the considerably more sophisticated quantum chemistry self-consistent-field (SCF) results of Ref. 36 who find 568 cm^{-1}.

In Fig. 4(a) are shown the eigenvalues of the one-electron LDA Hamiltonian for Si_2 as a function of Si-Si distance. The $1\pi_u$ electronic level is fourfold degenerate (including spin) and contains two electrons in equilibrium ($d=2.27$ Å). The $2\sigma_g$ level crosses the $1\pi_u$ level as the distance is decreased. This is in excellent agreement with the spin-polarized results of Northrup *et al.*,[38] who find that the $1\pi_u$ level crosses the doubly degenerate $2\sigma_g$ level at about $4.0a_B$ (2.12 Å), resulting in a new ground-state configuration at smaller separations. We also find the $1\pi_u$ level crossing the $2\sigma_g$ level at $d=2.12$ Å. This results in a potential-energy surface with two minima as shown in Fig. 4(b). A metastable configuration exists at $d\simeq 2.03$ Å.

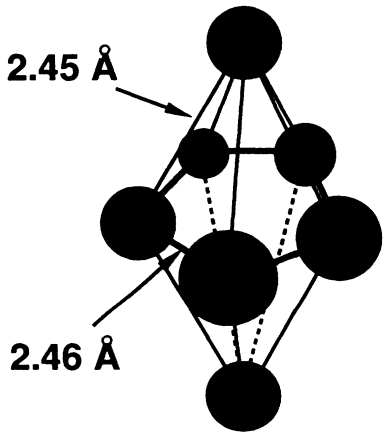

FIG. 15. Ground-state configuration of Si_7. This structure is a pentagonal bipyramid, consisting of a pentagon with one atom above the plane of the pentagon and one atom below.

B. Si_3

The Si_3 ground-state configuration we find by dynamical quenching is an isosceles triangle with the two equal sides of length $d=2.189$ Å and an opening angle of $\theta=78.8°$ (see Fig. 5). These results are in good agreement with the more rigorous quantum-chemistry SCF calculations of Diercksen *et al.*,[39] who find $d=2.196$ Å and $\theta=80.6°$. Grev *et al.*[40] who find $d=2.160$ Å and $\theta=78.1°$, and Raghavachari *et al.*[34] who find $d=2.17°$ and $\theta=77.8°$.

The energy eigenvalues as a function of the angle θ (with the distance d kept constant at its value at equilibrium) are shown in Fig. 6(a). The Fermi level lies between the sixth and seventh levels. These two levels become degenerate at $\theta=60°$ (an equilateral triangle), which make this geometry Jahn-Teller unstable. The total energy as a function of θ (again with d fixed) is shown in Fig. 6(b). Two equivalent minimum are seen corresponding to $\theta=78.8°$ and $\theta=281.2°$. The system is clearly unstable at 60°, and a relatively large barrier separates the two equivalent minimum as the molecule passes through 180°, where the molecule forms a linear chain as occurs for C_3. Curiously, we find a very shallow local minimum at the linear chain. This is to be contrasted to the SCF results of Raghavachari,[14] which find the linear chain to be unstable. The imaginary frequency found in that work ($82i$ cm^{-1}) is very small, indicating a relatively flat potential surface similar to ours.

The spectral density function $g(\omega)$ in the harmonic ($T_K=50$ K) and the near-harmonic ($T_K=500$ K) regions for Si_3 vibrations are shown in Fig. 7. Three peaks are apparent corresponding to the $3n-6$ normal modes of vibration. The width of the peaks is due to the finite time of the simulation. The position of the peaks indicates the frequency of the normal mode, while the relative heights reflect the (randomly chosen) relative amplitudes in each of the modes. The spectrum at low temperature is pure, indicating very little anharmonicity, while at higher temperatures, small contributions to anharmonic affects (sum and difference frequencies) are evident. Also notice the overall shift toward lower frequencies. The "harmonic" frequencies at 50 K are 202, 474, and 596 cm^{-1} for the A_1, B_2, and A_1 symmetric modes, respectively. These can be compared with those obtained by Grev *et al.*[40] of 157, 570, and 574 and Raghavachari[41] of 206, 560, and 582. We note that both of our A_1 modes are in good agreement with these quantum-chemistry SCF calculations, while the B_2 mode is only in fair agreement, with our mode lying $\sim 16\%$ lower than theirs. This is not unreasonable as typically calculated frequencies of molecules are accurate to $\sim 10-15\%$.[42]

The molecular-dynamics technique makes no assumptions about harmonic potentials and does not construct a dynamical matrix. Very harmonic systems are treated in exactly the same way as an anharmonic system. We show in Fig. 8 the results of a simulation of Si_3 at a very high temperature of ~ 2500 K. The simulation was of 3600 time steps and there is no indication that the molecule is about to disassociate. The motion is two dimensional and a snapshot of the motion is shown in Fig. 8(a). Within the chaotic motion, one sees a nearly sixfold pattern coming from a molecule containing only three atoms. This occurs because the atom that acts as the apex of the ground-state triangular molecule is being changed from one atom to the next. Also there is considerable classical tunnelinglike behavior of the apex atom through the center line connecting the other two atoms. The spectral density function $g(\omega)$ [Fig. 8(b)] has lost the three-peak structure of the harmonic system, and takes on a continuous spectrum. The frequencies depend on the amplitude of each of the "modes," and the amplitudes are continuously changing.

C. Si_4

The equilibrium configuration determined for Si_4 is a rhombus with side length 2.32 Å and a minor diagonal length of 2.39 Å (see Fig. 9). This compares very well with the results of Tománek and Schlüter,[14] who find a rhombus of side length 2.3 Å with a diagonal of 2.4 Å, and the results of Raghavachari and Logovinsky,[34] who also find a rhombus of side 2.30 Å and diagonal 2.40 Å. Other possible geometries include the square and tetrahedron. The square forms a metastable minimum-energy configuration with a side of length 2.32 Å, and the tetrahedron is metastable with minimum energy of side length 2.46 Å. The energies of these two structures are shown in Fig. 2 and are significantly higher in energy ($\simeq 0.61$ eV/atom and $\simeq 0.53$ eV/atom, respectively) than the rhombus.

The one-electron LDA energy eigenvalues are plotted as a function of the angle θ in Fig. 10(a). As in the case of Si_3, there is again a crossing of levels at the configuration of highest symmetry (in this case, $\theta = 90°$). This causes a Jahn-Teller unstable system that shows up as a cusp in the total energy per atom also as a function of the angle θ in Fig. 10(b).

The vibrational spectrum of Si_4 is shown in Fig. 11 for a high and low kinetic temperature. There are $3n-6=6$ normal modes for Si_4 and the high-temperature spectrum shows the mode-softening characteristic of anharmonicity at higher-excitation levels. The normal coordinates that give rise to the various peaks in the spectrum are labeled according to symmetry. The lowest frequency mode is B_{3u}, which is the "bond-bending" mode in which alternate atoms move out of and into the plane of the paper (see Fig. 9). The other bond-bending mode is B_{2u} in which the atoms move in the plane of the paper. The frequencies found from an examination of Fig. 11 are compared with those of Raghavichari and Rohlfing[43] in Table I. Overall agreement with these far more sophisticated calculations is excellent.

D. Si_5

We find the equilibrium structure of Si_5 based on annealing and quenching to be a trigonal bipyramid, consisting of an equilateral triangle of side 3.02 Å capped on top and bottom, with the distance between the corners of the triangle and a cap being 2.30 Å (see Fig. 12). This structure agrees with those found by Tománek and Schlüter,[14] who find a trigonal bipyramid with the relevant lengths of 3.1 and 2.4 Å, and Raghavachari and Logovinsky,[34] who find the same structure with distances of 2.34 and 3.26 Å. Metastable structures for Si_5 include the pentagon and pyramid. The energetics of these structures are shown in Fig. 2, where the pentagon is $\simeq 1.00$ eV/atom higher and the pyramid is $\simeq 0.13$ eV/atom higher.

The vibrational spectral density function of Si_5 is shown in Fig. 13 at low temperature ($T \simeq 50$ K). The five peaks in the figure come about because three frequencies are doubly degenerate, while an additional frequency is "accidentally" degenerate, and unresolvable.

E. Si_6

The equilibrium structure for Si_6 is that of a bipyramid, consisting of a square with side length 2.71 Å capped on top and bottom, with the distance between a vertex of the square and a cap being 2.36 Å (see Fig. 14). This structure agrees with that found by Tománek and Schlüter,[14] who also find such a "distorted octahedron" with the relevant distances of 2.6 and 2.3 Å. Raghavachari,[36] however, finds the ground-state structure to be an edge-capped trigonal bipyramid.

The energies of higher-energy metastable states for $n=6$ are shown in Fig. 2. Three structures investigated are structures higher in energy than the equilibrium structure: (1) a hexagon ($\simeq 1.22$ eV/atom higher in energy), (2) the singly capped pentagon ($\simeq 0.50$ eV/atom higher), and (3) a sixfold buckled ring which is a bulk fragment ($\simeq 0.22$ eV/atom higher).

F. Si_7

The ground-state structure found for Si_7 is a bicapped pentagon, consisting of a pentagon of side length 2.46 Å capped on top and bottom, with the distance between a vertex of the pentagon and a cap being 2.45 Å (see Fig. 15). This is in agreement with Ballone *et al.*,[44] who also find a pentagonal bipyramid as the equilibrium structure. In addition, when just dynamical quenching is performed, the system invariably settles into a capped and strongly reconstructed version of the sixfold buckled ring. This metastable structure is relatively close in energy ($\simeq 0.16$ eV/atom higher) to this equilibrium structure.

V. CONCLUSIONS

We have used an approximate electronic-structure method to determine the electronic and vibrational spectrum and the equilibrium structures of small Si clusters. The method used is a simplified *ab initio* tight-binding model based on local-density theory, and has no adjust-

able parameters. We have compared a number of our results with those of others and find substantial agreement with more rigorous calculations. Based on these results for small molecules, we are optimistic that the molecular-dynamics technique and energy functional used here will be applicable to bulk crystalline and amorphous covalent semiconductors and to semiconductor surfaces as well. The method is computationally fast and efficient, and should permit us to study covalent systems of previously incalculable complexity.

ACKNOWLEDGMENTS

Two of us (O.F.S. and D.J.N.) wish to thank the Office of Naval Research, U.S. Department of Defense, for their encouragement and support under Contract No. ONR-N00014-90-J-1304. Two others (D.A.D. and J.D.D.) wish to acknowledge support under Contracts No. AF-AFOSR-89-0063 and No. ONR-N00014-89-J-1136. We wish to thank Gary Adams and Stefan Klemm for their insights, helpful comments, and suggestions.

[1]E. Pearson, T. Takai, T. Halicioglu, and W. A. Tiller, J. Cryst. Growth **70**, 33 (1984); T. Takai, T. Halicioglu, and W. A. Tiller, Scr. Metall. **19**, 709 (1985).

[2]F. H. Stillinger and T. A. Weber, Phys. Rev. B **31**, 5262 (1985).

[3]M. I. Biswas and D. R. Hamann, Phys. Rev. Lett. **55**, 2001 (1985); R. Biswas and D. R. Hamann, Phys. Rev. B **36**, 6434 (1987).

[4]D. W. Brenner and B. J. Garrison, Phys. Rev. B **34**, 1304 (1986).

[5]J. Tersoff, Phys. Rev. Lett. **56**, 632 (1986); Phys. Rev. B **37**, 6991 (1988); **38**, 9902 (1988).

[6]M. I. Baskes, Phys. Rev. Lett. **59**, 2666 (1987); B. W. Dodson, Phys. Rev. B **35**, 2795 (1987).

[7]J. Chelikowsky, J. C. Phillips, M. Kamal, and M. Strauss, Phys. Rev. Lett. **62**, 292 (1989).

[8]G. Ackland, Phys. Rev. B **40**, 10 351 (1989).

[9]A. Carlsson, P. A. Fedders, and C. W. Myles, Phys. Rev. B **41**, 1247 (1990).

[10]K. E. Khor and S. Das Sarma, Phys. Rev. B **40**, 1319 (1989).

[11]B. C. Bolding and H. C. Andersen, Phys. Rev. B (to be published).

[12]J. R. Chelikowsky, J. C. Phillips, M. Kamal, and M. Strauss, Phys. Rev. Lett. **62**, 292 (1989); J. R. Chelikowsky and J. C. Phillips, *ibid.* **63**, 1653 (1989).

[13]D. J. Chadi, Phys. Rev. B **29**, 785 (1985); Phys. Rev. Lett. **59**, 1691 (1987); G. X. Xian and D. J. Chadi, Phys. Rev. B **35**, 1288 (1987).

[14]D. Tománek and M. A. Schlüter, Phys. Rev. B **36**, 1208 (1987).

[15]D. G. Pettifor, A. J. Skinner, and R. A. Davies, in *Atomistic Simulation of Materials—Beyond Pair Potentials,* edited by V. Vitek and D. J. Srolovitz (Plenum, New York, 1989), p. 317; A. P. Sutton, M. W. Finnis, D. G. Pettifor, and Y. Ohta, J. Phys. C **21**, 35 (1988).

[16]A. T. Paxton and A. P. Sutton, J. Phys. C **21**, L481 (1988); A. T. Paxton, A. P. Sutton, C. M. M. Nex, *ibid.* **20**, L263 (1987); A. T. Paxton, *Atomistic Simulation of Materials—Beyond Pair Potentials,* edited by V. Vitek and D. J. Srolovitz (Plenum, New York, 1989), p. 265.

[17]J. A. Majewski and P. Vogl, Phys. Rev. Lett. **57**, 1366 (1986).

[18]J. R. Chelikowsky and R. Redwing, Solid State Commun. **64**, 843 (1987).

[19]O. F. Sankey and R. E. Allen, Phys. Rev. B **33**, 7164 (1986).

[20]R. E. Allen and M. Menon, Phys. Rev. B **33**, 5611 (1986); M. Menon and R. E. Allen, *ibid.* **33**, 7099 (1986); M. Menon and R. E. Allen, Superlatt. Microstruct. **3**, 295 (1987); M. Menon and R. E. Allen, Solid State Commun. **64**, 53 (1987).

[21]C. Z. Wang, C. T. Chan, and K. M. Ho, Phys. Rev. B **39**, 8586 (1989).

[22]F. S. Khan and J. Q. Broughton, Phys. Rev. B **39**, 3688 (1989).

[23]O. F. Sankey and D. J. Niklewski, Phys. Rev. B **40**, 3979 (1989); in *Atomistic Simulation of Materials—Beyond Pair Potentials,* edited by V. Vitek and D. J. Srolovitz (Plenum, New York, 1989), p. 95.

[24]W. M. Foulkes and R. Haydock, Phys. Rev. B **39**, 12 520 (1989).

[25]D. M. Ceperley and G. J. Adler, Phys. Rev. Lett. **45**, 566 (1980). These numerical results have been parametrized by J. Perdew and A. Zunger, Phys. Rev. B **23**, 5048 (1981).

[26]D. R. Hamann, M. Schlüter, and C. Chiang, Phys. Rev. Lett. **43**, 1494 (1979).

[27]J. Harris, Phys. Rev. B **31**, 1770 (1985).

[28]H. M. Polatoglou and M. Methfessel, Phys. Rev. B **37**, 10 403 (1988).

[29]A. J. Read and R. J. Needs, J. Phys. Condens. Matter **1**, 7565 (1989).

[30]C. W. Gear, Argonne National Laboratory Report No. ANL-7126, 1966 (unpublished); Y. H. Lee, Ph.D. thesis, Kent State University, 1986.

[31]S. Kirkpatrick, C. D. Gellatt, Jr., and M. P. Vecchi, Science **220**, 671 (1983).

[32]M. Metropolis, A. W. Rosenbluth, M. N. Rosenbluth, A. H. Teller, and E. Teller, J. Chem. Phys. **21**, 1087 (1953).

[33]F. J. Harris, Proc. IEEE **66**, 51 (1978).

[34]K. Ragavachari and V. Logovinsky, Phys. Rev. Lett. **55**, 2853 (1985).

[35]The increase of kinetic energy due to the compact orbitals is much smaller for clusters and solids, due to hopping amongst the atoms, than it is for the isolated atom.

[36]K. Raghavachari, J. Chem. Phys. **84**, 5672 (1986).

[37]D. E. Milligan and M. E. Jacox, J. Chem. Phys. **52**, 2594 (1970), and references therein.

[38]J. E. Northrup, M. T. Yin, and M. L. Cohen, Phys. Rev. A **28**, 1945 (1983).

[39]G. H. F. Diercksen, N. E. Gruner, J. Oddershele, and J. R. Sabin, Chem. Phys. Lett. **117**, 29 (1985).

[40]R. S. Grev and H. F. S. Schaefer, Chem. Phys. Lett. **119**, 111 (1985).

[41]K. Raghavachari, J. Chem. Phys. **83**, 3520 (1985).

[42]J. A. Pople, H. B. Schlegel, R. Krishnan, D. J. Defrees, J. S. Brinkley, M. J. Frisch, and R. A. Whiteside, Int. J. Quantum Chem. Symp. **15**, 269 (1981).

[43]K. Raghavachari and C. M. Rohlfing, J. Chem. Phys. **89**, 2219 (1988).

[44]P. Ballone, W. Andreoni, R. Car, and M. Parrinello, Phys. Rev. Lett. **60**, 271 (1988).